NACA RM E54I14

NACA

RESEARCH MEMORANDUM

EFFECTIVENESS OF BOUNDARY-LAYER REMOVAL NEAR THROAT OF RAMP-TYPE SIDE INLET AT FREE-STREAM MACH NUMBER OF 2.0

By Leonard J. Obery and Robert W. Cubbison

Lewis Flight Propulsion Laboratory
Cleveland, Ohio

CLASSIFIED DOCUMENT

NATIONAL ADVISORY COMMITTEE
FOR AERONAUTICS

WASHINGTON

November 17, 1954

NACA RM E54I14

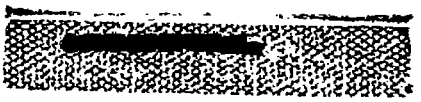

NATIONAL ADVISORY COMMITTEE FOR AERONAUTICS

RESEARCH MEMORANDUM

EFFECTIVENESS OF BOUNDARY-LAYER REMOVAL NEAR THROAT OF RAMP-TYPE SIDE INLET AT FREE-STREAM MACH NUMBER OF 2.0

By Leonard J. Obery and Robert W. Cubbison

SUMMARY

The effect of removal of the boundary layer inside the inlet (in addition to removal of the fuselage boundary layer) on the performance of a twin-duct side-air-intake system was investigated in the Lewis 8- by 6-foot supersonic wind tunnel at a free-stream Mach number of 2.0. The boundary layer formed on the external-compression surfaces was removed near the inlet throat either by a flush slot or by one of several ram scoops. The experimental results indicated that internal boundary-layer bleed could improve the pressure recovery sufficiently to effect a gain in propulsive thrust despite the drag penalty associated with boundary-layer removal. Although all bleed inlets exhibited higher total-pressure recoveries than the no-bleed inlet, the greatest gains in critical total-pressure recovery and also in propulsive thrust occurred with the least amount of bleed, indicating that only the lowest energy air need be removed from the inlet. The stable subcritical mass-flow range was increased from 10 percent with the ram-scoop inlet to 18 percent with the flush-slot inlet for comparable boundary-layer removal; however, peak total-pressure recovery was not affected by the method of boundary-layer bleed.

INTRODUCTION

The performance characteristics of a twin-duct side-air-intake system mounted on a fuselage forebody with complete fuselage boundary-layer removal were investigated in the NACA Lewis 8- by 6-foot supersonic wind tunnel and reported in reference 1. During that investigation, a pitot-pressure survey near the inlet throat revealed a thick boundary layer flowing downstream from the compression ramps. This boundary layer occupied about 10 percent of the inlet flow area. In addition to its intrinsically low pressure recovery, interaction between the boundary layer and the main duct flow may be expected to cause adverse effects on the subsonic diffusion process. Another investigation (ref. 2) on a smaller

inlet with a single external-compression ramp also showed an undesirable boundary layer formed on the compression surfaces. In this case, interaction with the inlet terminal shock had caused boundary-layer separation from the ramp. Therefore, several investigations were conducted to determine possible gains in diffuser performance that could be attained by bleeding the ramp boundary layer from the inlet before subsonic diffusion.

For the investigation on the smaller single-wedge inlet, ram scoops of various heights were used to remove the internal boundary layer. The results of that investigation are presented in reference 3. The present investigation incorporated either ram scoops of various heights or a flush slot located just downstream of the cowl lip to remove the inlet boundary layer. The effect of internal boundary-layer bleed on over-all diffuser performance, total-pressure distribution at the diffuser exit, and net propulsive thrust at a free-stream Mach number of 2.0 are presented in this report.

SYMBOLS

The following symbols are used in this report:

A	area
D	drag
F	thrust of J67-W-1 engine when operated behind an inlet at a particular total-pressure recovery
h	height at lip of ram scoop
L	length of subsonic diffuser, 81.5 in.
M	Mach number
m_3/m_0	mass-flow ratio, $\frac{\text{mass flow}}{\rho_0 V_0 A_1}$
$(m_3/m_0)_{max}$	maximum-capture mass-flow ratio of any inlet
$(m_3/m_0)_{min}$	minimum value of stable mass-flow ratio of any inlet
P	total pressure
p	static pressure
V	velocity

[redacted]

x	distance from cowl lip, model station 36
$\frac{\Delta m_3}{m_0}$	ratio of amount of mass flow removed by bleed to $\rho_0 V_0 A_1$
δ	boundary-layer height at inlet throat, 0.25 in.
ρ	mass density of air

Subscripts:

b	boundary-layer bleed
c	critical
n	no-bleed inlet
x	conditions at x-distance from cowl lip
0	free stream
3	diffuser-exit survey station, model station 100

Pertinent areas:

A_1	projected frontal area of both inlets, 0.3646 sq ft
A_t	inlet throat area of both ducts, 0.228 sq ft
A_3	flow area at diffuser discharge, 0.457 sq ft

APPARATUS AND PROCEDURE

The model of the present investigation is illustrated photographically in figure 1 and schematically in figure 2. Shown in these figures are the twin double-ramp side inlets mounted on the 1/4-scale fuselage forebody of a supersonic airplane. The ducts were geometrically similar and joined into a common duct at a model station which corresponded to the engine compressor face.

The model was sting-mounted in the tunnel with no provisions to obtain force measurements. The dark extension to the fuselage, which can be seen in figure 1, was a shroud used to protect various mechanisms. The reverse scoop seen in figure 1 was one of two mounted on the shroud to lower the pressure at the base of the model and ensure choking at the mass-flow control plug.

Details of the model, including internal flow stations and representative model cross sections, are shown in figure 2. The nose of the model was canted down at an angle of 5°, and the inlets were canted at an angle of 3°, both with respect to the fuselage center line. The 5° droop of the nose was intended to facilitate pilot vision in the prototype rather than to influence flow conditions for maximum performance.

Photographs and schematic drawings of the inlets are shown in figure 3. The inlet had a 9° first compression ramp and an 18° second compression ramp. The leading edge of the first ramp was positioned so that the resulting oblique shock was located just ahead of the cowl lip at a Mach number of 2.0. The first ramp also acted as a boundary-layer splitter plate and completely removed the fuselage boundary layer. Figure 3(a) shows the no-bleed inlet, that is, the inlet which had no boundary-layer bleed apparatus. The shape of the wall aft of the compression ramps was formed by removable contoured blocks. Three ram-scoop heights of 1/8, 1/4, and 1/2 inch corresponding approximately to 1/2, 1, and 2 boundary-layer thicknesses, respectively, were investigated. These changes were made by inserting spacers under the blocks as shown in figure 3(c). The no-bleed inlet and the flush-slot inlet were designed to have a length of approximately three hydraulic diameters of nearly constant-area section before subsonic diffusion (fig. 4), with approximately $1\frac{1}{2}$ percent of area expansion per hydraulic diameter provided to allow for boundary-layer growth. The ram-scoop configurations were designed to the same criterion, provided a stream tube with height equal to the boundary-layer inlet height entered the ram scoops. No throttling of the bleed air flow was attempted other than that resulting from choking at the bleed inlet throat. Choking undoubtedly occurred in the bleed throat because the pressure inside the fuselage, into which the bleed air initially discharged, was less than free-stream static, resulting in a pressure ratio in excess of 5.0 across the gap.

The model instrumentation was identical to that of reference 1 except that total-pressure rakes in the inlet ducting at station 40 and the boundary-layer total-pressure rakes were not used. No force measurements were made during this investigation. Except for the fuselage boundary-layer mass flow, the computational methods were also identical to those described in reference 1.

The investigation was conducted at a free-stream Mach number of 2.0 and at a fuselage angle of attack of $3\frac{1}{2}^\circ$, corresponding to an inlet angle of attack of about 0°. The Reynolds number for the investigation was approximately 4.25×10^6 per foot of length.

RESULTS AND DISCUSSION

The internal performance characteristics of the various inlets are presented in figure 5. The no-bleed inlet is similar to the inlet reported in reference 1; however, the supercritical mass-flow ratio is lower, while the critical and peak total-pressure recoveries are higher than those of the previous investigation. The difference in characteristics probably results from a slight forward shift of the second-ramp leading edge. This forward shift probably eliminated the region of the low external-compression flow reported in reference 1 and thus increased the supersonic-diffusion total-pressure recovery. Because of the forward movement of the second shock, a lower maximum-capture mass-flow ratio would be expected.

The difference in supercritical mass-flow ratio between the various bleed inlets and the no-bleed inlet (as shown in fig. 5) represents the amount of mass flow removed by the inlet boundary-layer bleed openings. The amount of mass flow removed progressively increased with bleed-gap minimum area for the ram-scoop configurations, as shown in figure 6. The difference between the theoretical curve (calculated for choking at bleed minimum area at measured total-pressure recovery ahead of the bleed inlet) and the experimental data points probably results from the flow coefficient of the bleed inlet. The marked difference in flow coefficient between the ram-scoop and the flush-slot configurations is also evident; the ram-scoop inlets indicate about a 90-percent effective area as compared with about 40 percent for the flush-slot configuration. The low mass flow in the boundary layer is also apparent; for example, with the highest ram scoop, an area of about 23 percent of the duct throat area was required to bleed 16 percent of the duct mass flow.

As shown in figure 7, the diffuser total-pressure recovery at critical inlet flow increased rapidly as a small amount of boundary-layer mass flow was bled from the inlet. The highest critical pressure recovery occurred with about 3 to 4 percent bleed, corresponding to removal of about 1/2 the inlet boundary layer. Peak total-pressure recovery also increased rapidly with small amounts of bleed but remained relatively constant with increasing amounts of removal. For comparable amounts of boundary-layer removal, the manner of bleeding the boundary layer (either with ram scoops or the flush slot) had little effect on critical total-pressure recovery. The amount of inlet stability, however, was markedly affected by the type bleed as shown in figure 7 where, for 3 to 4 percent mass-flow bleed, the stable subcritical range was increased from 10 percent with the ram-scoop inlet to 18 percent with the flush-slot inlet. Since the area variations along the initial diffuser length are identical (for a streamline of ram-scoop height entering the scoop) and all other diffuser parts were common to both systems, no explanation for the extended range is evident. As also shown in figure 7, as the ram-scoop

height was raised from $h/\delta = 0$ to 2.0, the stable range at first decreased and then increased to a value greater than that for the no-bleed configuration.

Bleeding the inlet boundary layer also tended to improve the total-pressure distribution at the diffuser exit (fig. 8). For the no-bleed inlet, areas of high total-pressure recovery tended to form behind both inlets at critical mass-flow ratio (fig. 8(a)) or behind only one inlet for very subcritical values (fig. 8(b)). In either case, the compressor blades would be subjected to periodic changes in total-pressure levels during each revolution of the engine. Bleeding the inlet boundary layer with the flush scoop had little effect on the distribution at critical inlet flow (fig. 8(c)), but for subcritical flow (fig. 8(d)) the concentrated areas of high total-pressure recovery tended to spread into an annular shape. This tendency is even more pronounced for the ram-scoop configurations (figs. 8(e) and (f)). For the bleed configurations, differences on the order of 2 percent in total-pressure recovery occurred across the compressor face for subcritical mass-flow ratios (figs. 8(d) and (f)).

An analysis was made to determine the approximate over-all effect of bleeding the inlet boundary layer on the performance of the inlet-engine combination. In figure 9 the thrust minus drag of each configuration was referenced to the thrust of the inlet-engine combination at critical inlet flow for the no-bleed inlet when matched to the J67-W-1 engine at a free-stream Mach number of 2.0. This parameter was plotted against a mass-flow ratio, which is defined as the ratio of the mass flow of an inlet (at any point in its stable regulation range) to the critical mass-flow ratio of the no-bleed inlet. The matching of the inlets at any point in the mass-flow-ratio range was accomplished by sizing the inlet area so that operation would occur at the desired mass-flow ratio. The inlet size thus would become progressively larger as the operating mass-flow ratio became smaller.

In this analysis the following assumptions were made:

(1) The drag coefficient of the entire forebody does not change if the inlets are increased in size to accommodate the higher pressure recoveries and high quantities of mass flow bled from the inlet. This assumption was based on the data of references 1 and 4, which show that a 50-percent increase in inlet size did not increase the forebody drag when this drag was extrapolated to a mass-flow ratio of 1.0 in all cases.

(2) The mass flow removed by the inlet boundary-layer bleed will add drag to the inlet in the order of bypass spillage drag. This drag term was computed as the loss in momentum from free stream to sonic discharge at a total-pressure recovery equal to that of the diffuser and a discharge angle of about 15°. In an actual installation the bled

air might be discharged normal to the flight direction; in that case, a complete loss of momentum and a higher drag would result, or the air might be used for other aircraft purposes such as cooling, where no drag would be charged to the inlet.

(3) The subcritical drag rise for any of the inlets will be the same as the drag rise measured in reference 1. Operation in the subcritical range for any of the bleed inlets will then be penalized by drag resulting from internal boundary-layer bleed plus drag incurred by subcritical inlet spillage. Throughout the calculation it was assumed that the bleed mass flow remained constant in the inlet subcritical mass-flow range at the supercritical value and that all reduction from critical flow was accomplished by normal-shock spillage.

3448

All inlets showed an improvement in propulsive thrust over the no-bleed inlet at some part of their mass-flow range (fig. 9). The largest gains, however, resulted from the smallest amount of bleed (flush-slot inlet and ram-scoop inlet with $h/\delta = 0.5$). This trend resulted from the higher critical pressure recovery (fig. 5) and the low-drag increments associated with small amounts of bleed. Apparently then, to obtain maximum benefit, only the lowest energy air in the boundary layer should be removed from the inlet. The curves also indicate an interesting method of efficient inlet-engine matching at reduced flows. It is apparent that, with a variable-area bleed system, the inlet could have operated at 70 percent of the no-bleed inlet flow at an efficiency only slightly less than maximum for the no-bleed inlet.

SUMMARY OF RESULTS

The effect of removing the inlet boundary-layer air on the performance of a twin-duct side-air-intake system mounted on a fuselage forebody was investigated in the 8- by 6-foot supersonic wind tunnel at a free-stream Mach number of 2.0. The boundary layer produced on the compression ramps was removed near the inlet throat either by a flush slot or by one of several ram scoops. The following results were obtained:

1. Removal of the inlet boundary layer by an internal bleed can improve the diffuser total-pressure recovery sufficiently to offset the added spillage drag and produce a gain in propulsive thrust.

2. Higher peak total-pressure recoveries were obtained from the inlets with internal boundary-layer removal than with the no-bleed inlet, regardless of the type or the amount of removal.

3. The greatest gains in critical total-pressure recovery and in propulsive thrust resulted from the smallest amount of removal. The best bleed systems removed about 3 to 4 percent of the inlet mass flow or less than 50 percent of the inlet boundary layer.

4. The type of boundary-layer-removal system had a significant effect on the inlet stability limits. The stable subcritical mass-flow range was increased from about 10 percent with the ram-scoop inlet to 18 percent with the flush-slot inlet for comparable boundary-layer mass-flow removal.

Lewis Flight Propulsion Laboratory
National Advisory Committee for Aeronautics
Cleveland, Ohio, September 14, 1954

REFERENCES

1. Obery, Leonard J., Stitt, Leonard E., and Wise, George A.: Evaluation at Supersonic Speeds of Twin-Duct Side-Intake Systems with Two-Dimensional Double-Shock Inlets. NACA RM E54C08, 1954.

2. Campbell, Robert C., and Kremzier, Emil J.: Performance of Wedge-Type Boundary Layer Diverters for Side Inlets at Supersonic Speeds. NACA RM E54C23, 1954.

3. Campbell, Robert C.: Performance of a Supersonic Ramp Inlet with Internal Boundary-Layer Scoop. NACA RM E54I01, 1954.

4. Davids, Joseph, and Wise, George A.: Investigation at Mach Numbers 1.5 and 1.7 of Twin-Duct Side Intake System with Two-Dimensional 6° Compression Ramps Mounted on a Supersonic Airplane. NACA RM E53H19, 1953.

Figure 1. - Photograph of model.

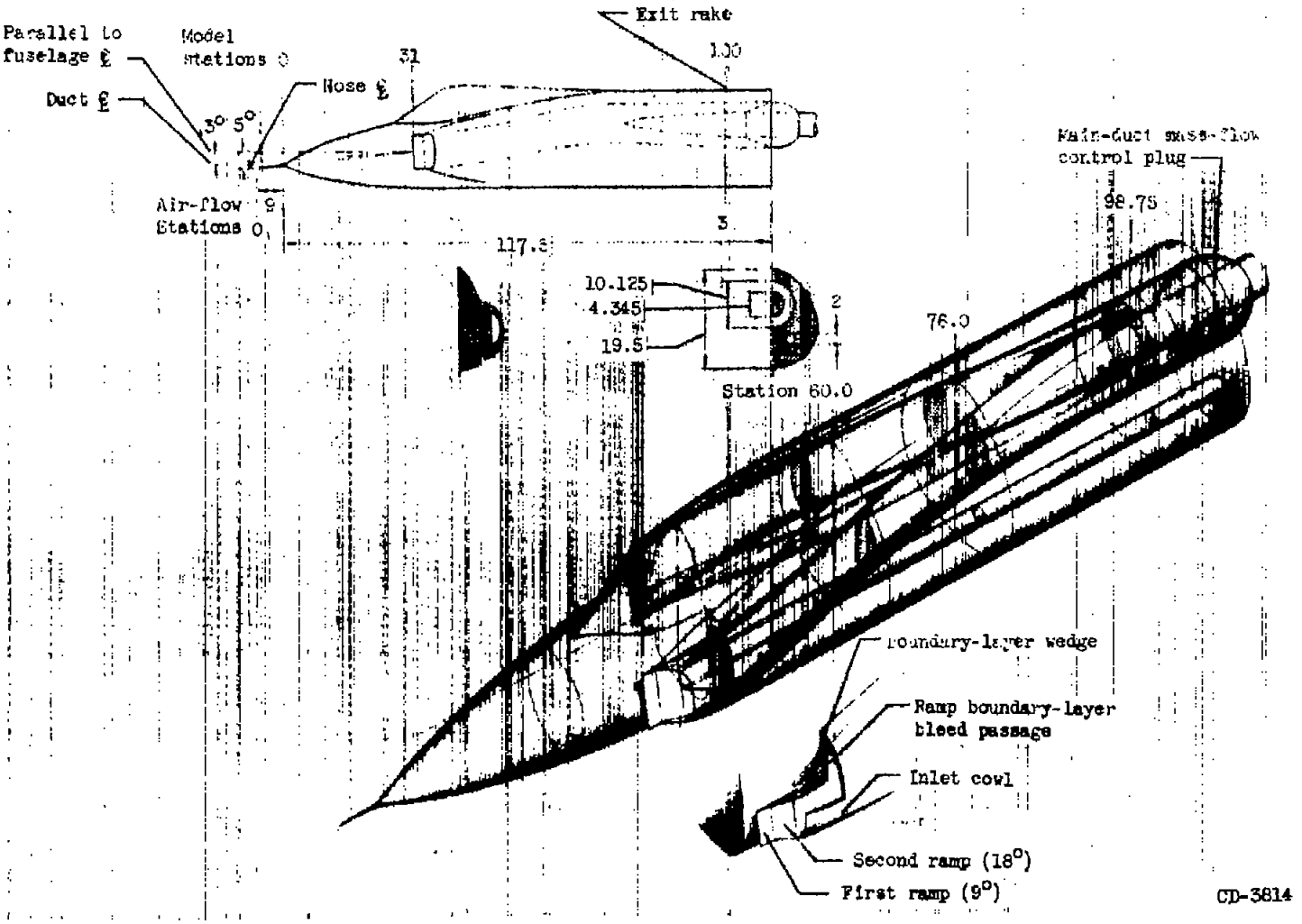

Figure 2. - Diagram of model with representative cross sections (all dimensions in inches).

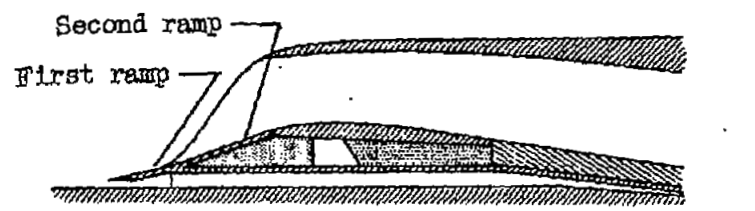

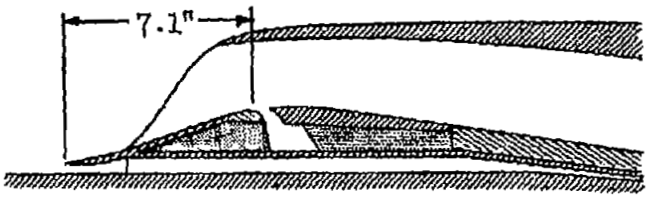

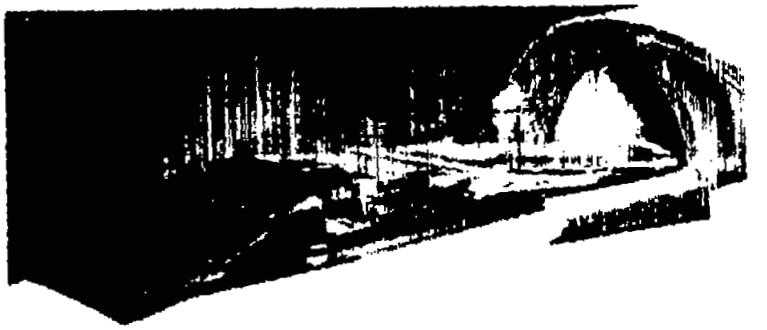

(a) No-bleed inlet.

(b) Flush-slot inlet.

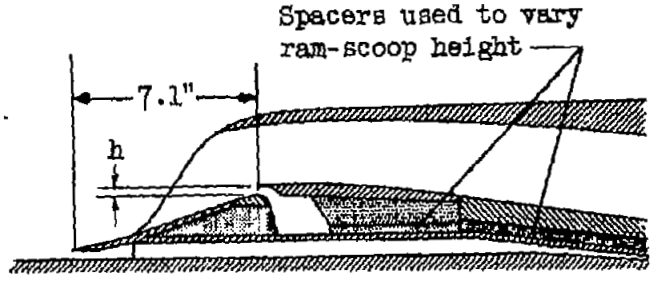

(c) Ram-scoop inlet.

C-36680
CD-3813

Figure 3. - Schematic drawings and photographs of various inlets.

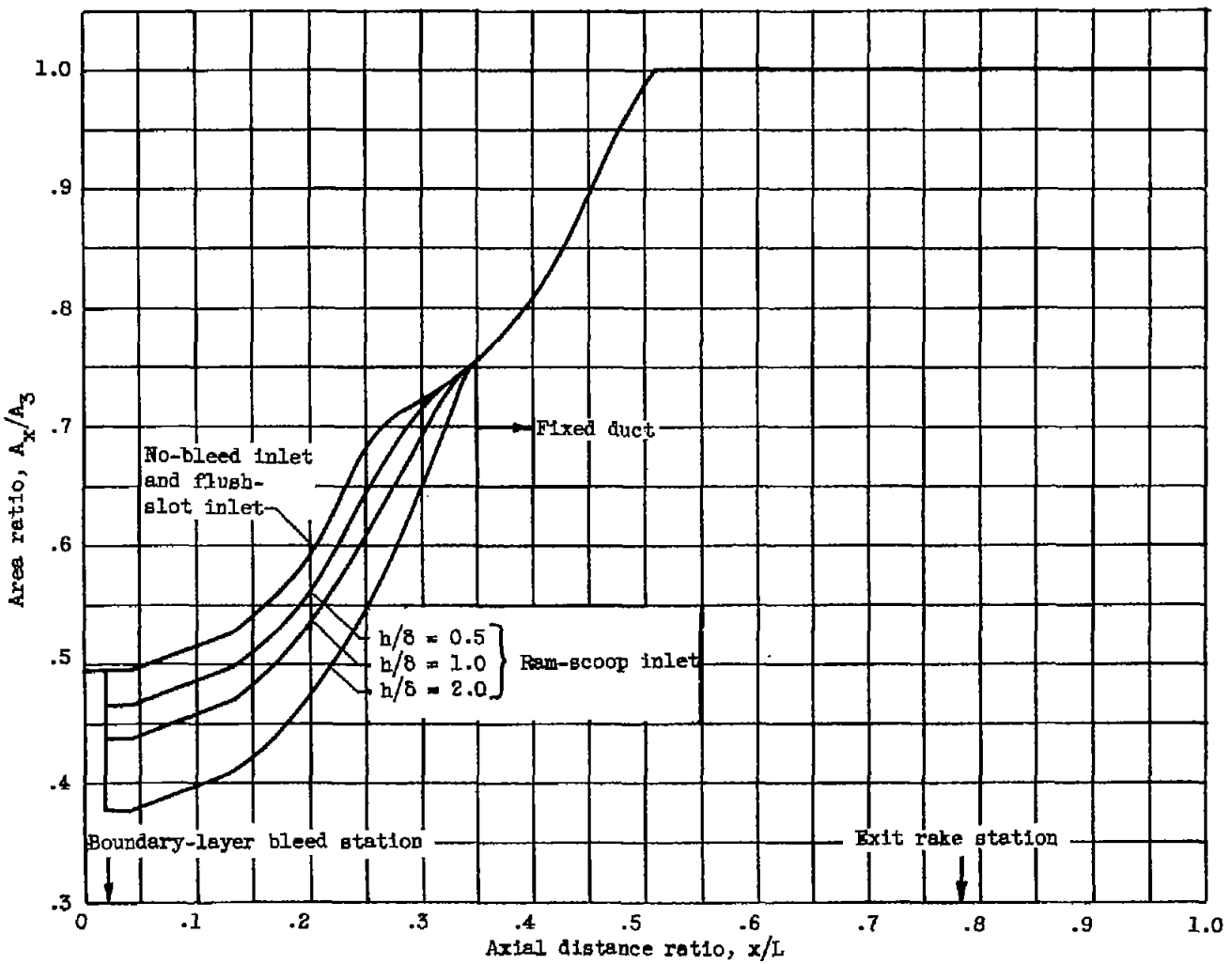

Figure 4. - Subsonic-diffuser area variation. Length of subsonic diffuser, L, 81.5 inches; flow area at diffuser discharge, A_3, 0.457 square feet.

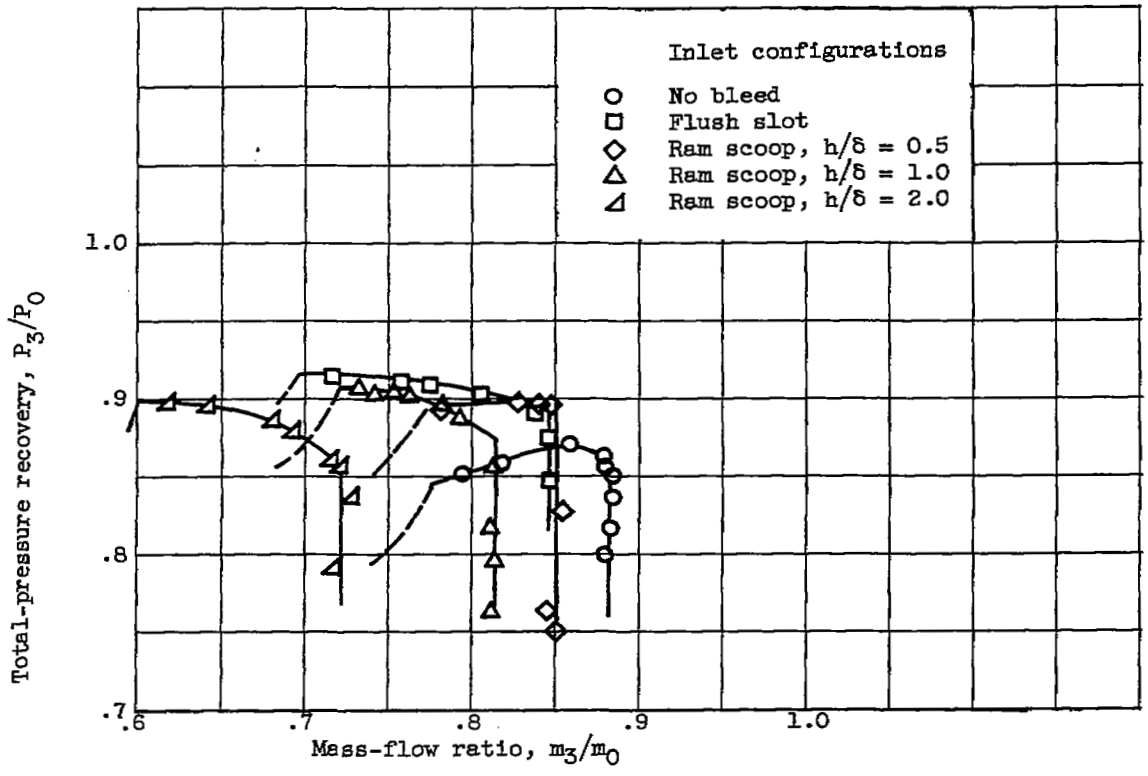

Figure 5. - Internal performance characteristics. Free-stream Mach number, 2.0; angle of attack, $3\frac{1}{2}^\circ$.

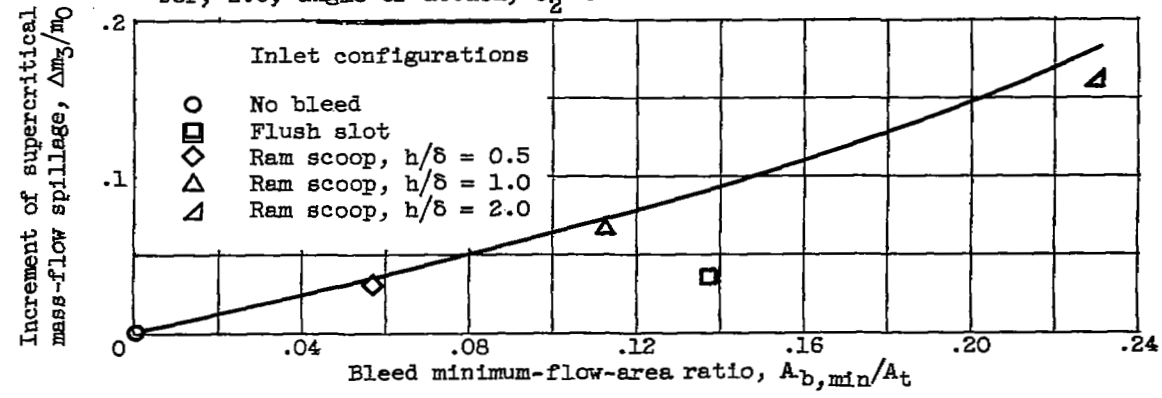

Figure 6. - Experimental and theoretical spillage through inlet bleed openings. Curve represents theoretical maximum spillage; symbols represent actual spillage.

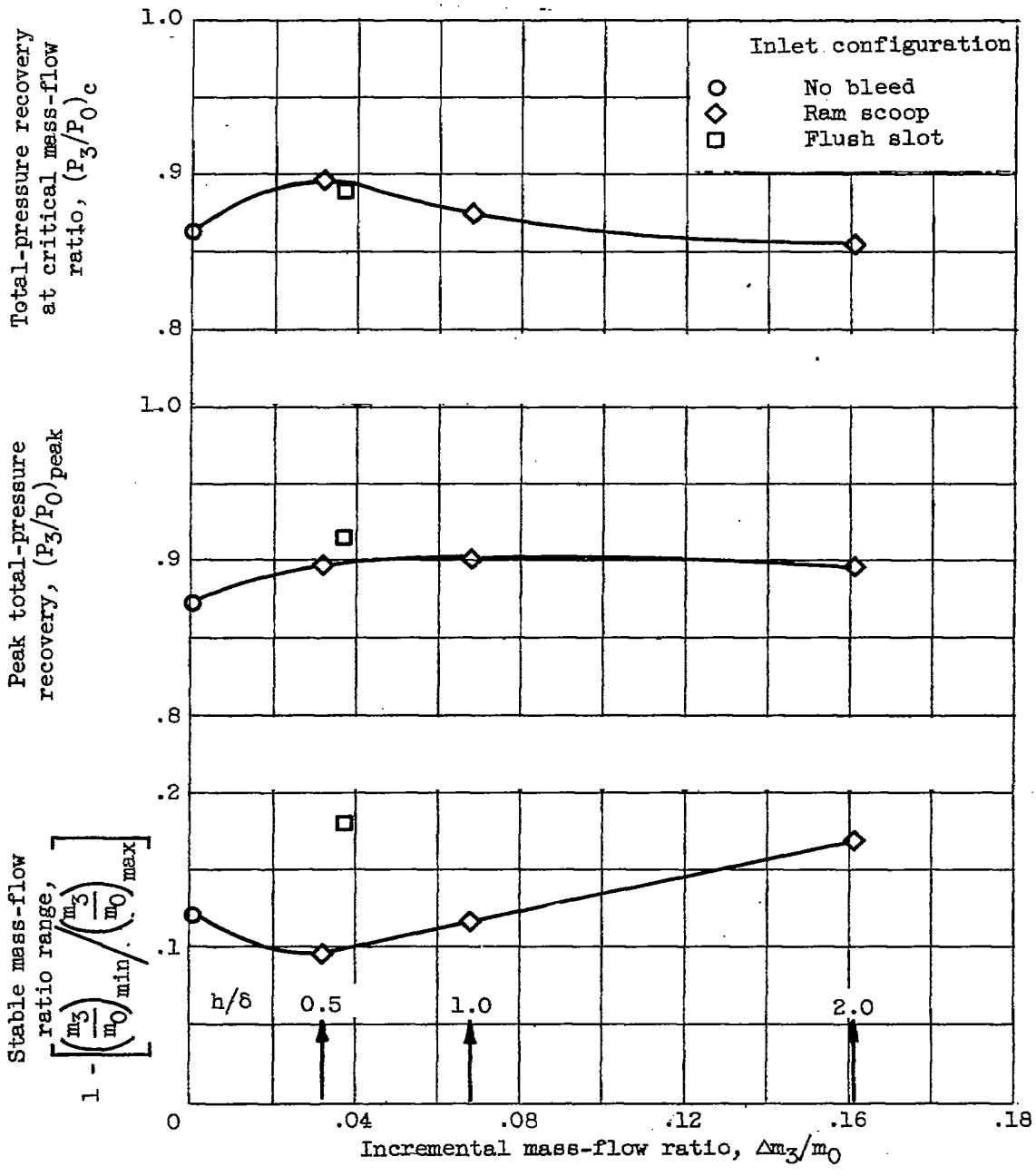

Figure 7. - Variation of particular internal performance characteristics for several configurations. Free-stream Mach number, 2.0.

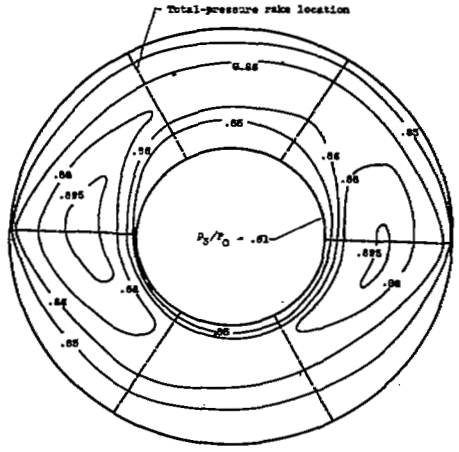

(a) No-bleed inlet; mass-flow ratio, 0.88; total-pressure recovery, 0.862.

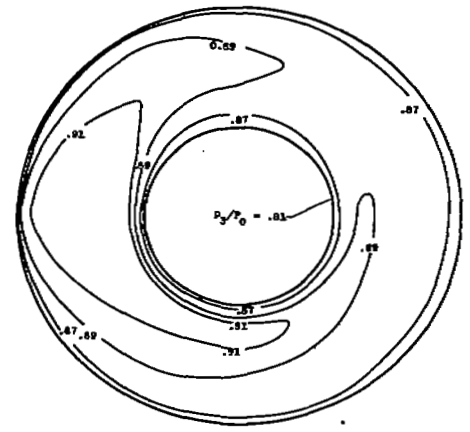

(b) No-bleed inlet; mass-flow ratio, 0.796; total-pressure recovery, 0.85.

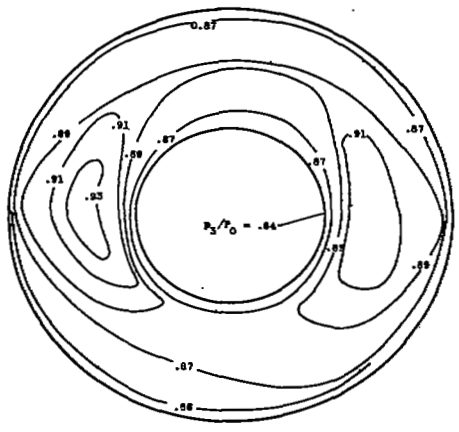

(c) Flush-slot inlet; mass-flow ratio, 0.836; total-pressure recovery, 0.889.

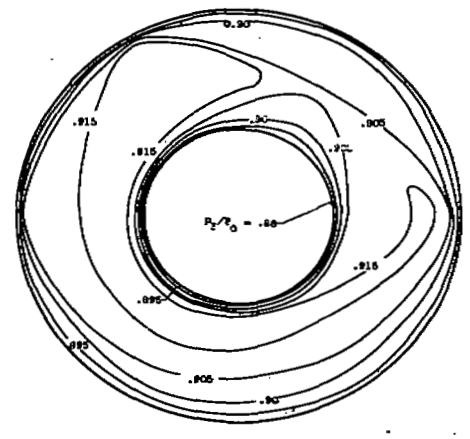

(d) Flush-slot inlet; mass-flow ratio, 0.716; total-pressure recovery, 0.914.

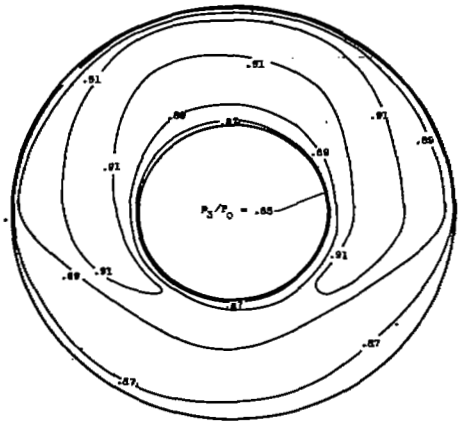

(e) Ram-scoop inlet (h/δ = 0.5); mass-flow ratio, 0.845; total-pressure recovery, 0.895.

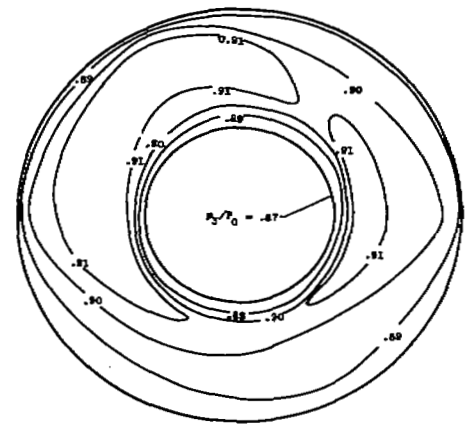

(f) Ram-scoop inlet (h/δ = 0.5); mass-flow ratio, 0.782; total-pressure recovery, 0.89.

Figure 8. - Total-pressure-recovery contours at diffuser exit.

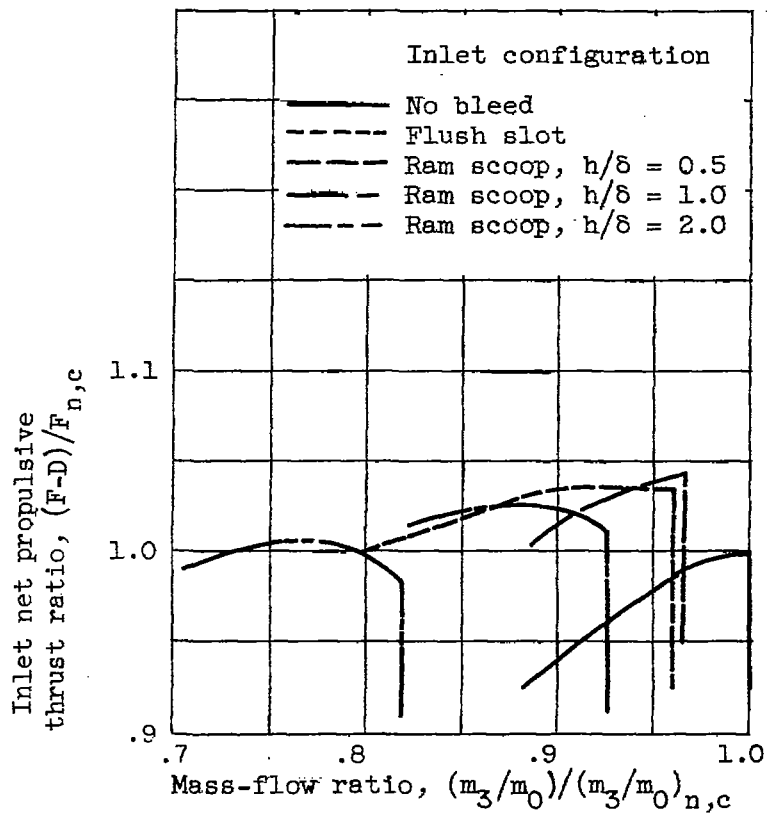

Figure 9. - Comparison of net propulsive thrust for various inlets.